

# Dielectric Waveguide Based Multi-Mode sub-THz Interconnect Channel for High Data-Rate High Bandwidth-Density Planar Chip-to-Chip Communication

Bo Yu, Yu Ye, Xuan Ding, Xiaoguang Liu, Jane Gu

**Abstract**— This paper presents a dielectric waveguide based multi-mode sub-THz interconnect channel for high data-rate high bandwidth-density planar chip-to-chip communications. By using a proposed new transition of microstrip line to dielectric waveguide, the interconnect channel achieves low insertion loss and wide bandwidth on two orthogonal modes  $E_{y11}$  and  $E_{x11}$ . To the authors' knowledge, this is the first demonstration of a multi-mode sub-THz interconnect channel. The measured minimum insertion losses for mode  $E_{y11}$  and mode  $E_{x11}$  are 8.0 dB with 21.3 GHz 3-dB bandwidth and 9.0 dB with 24.0 GHz 3-dB bandwidth, respectively.

**Index Terms**—Channel, chip-to-chip, communication, dielectric waveguide, interconnect, micromachined, multi-mode transition, orthomode transition, microstrip line, sub-THz, THz.

## I. INTRODUCTION

The demands of scientific workloads and commercial applications double increase the growth of the I/O bandwidth of intra/inter- chip communications every two years, and it would keep an upward trend in the future [1]. Nevertheless, physical constraints slow down the growth rate of the number of I/O pins and form an increasing gap, which limits the data rate per I/O area, defined as bandwidth density. Besides, the energy wasted in the data transmission would significantly be higher than that used for processing and storage [2]. With these two issues, both energy efficiency and bandwidth density of the interconnect should be boosted.

Interconnect research has been widely investigated in the optical and electrical areas. Optical interconnects have the advantages of low loss and wide bandwidth while the integration of high-efficient light sources with current CMOS processes is still very challenging. Electrical interconnects have the merits of compatibility and scalability with silicon processes while the different electrical schemes have their own restrictions on transmission loss, EM interferences, etc.

To boost both energy efficiency and bandwidth density, sub-THz/THz interconnect, using the spectrum sandwiched between optical and microwave frequencies, holds high potentials to fill the interconnect gap by leveraging advantages of both optical and electrical interconnect approaches: low-loss quasi-optical channels as well as advanced high-speed semiconductor devices.

The key components of the sub-THz/THz interconnect is dielectric waveguide (DWG) based channel and the transition from the microstrip line (MSL) to DWG. With the considerations of low loss and fabrication compatibility, the high resistivity silicon (HRS) is used as the transmission medium. The low-loss wide bandwidth channel has been

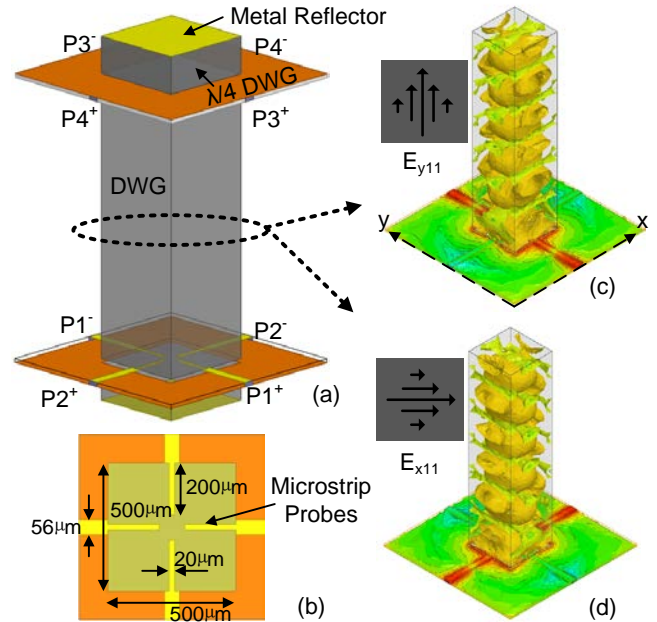


Fig. 1. Proposed DWG based multi-mode sub-THz interconnect channel. (a) Perspective view, (b) cross-section view of the transition interface with labeled dimensions, (c) the magnitude of E-field distribution of the mode  $E_{y11}$ , and (d) the magnitude of E-field distribution of the mode  $E_{x11}$ . studied in [3], [4].

To further boost the data rate and bandwidth density, the multi-mode channel, consisting of the multi-mode waveguide and the multi-mode transitions, is an attractive candidate. The simplest multi-mode channel is known as the orthomode channel, which consists of a square waveguide and two orthomode transition/transducer (OMT). The OMT combines or separates two signals with orthogonal polarization. The conventional orthomode channels [5], [6] are built by metallic waveguide, which occupies a large transition area and is challenging to integrate with planar processes.

This paper presents a DWG based multi-mode sub-THz interconnect channel for high data-rate high bandwidth-density planar chip-to-chip communications, as shown in Fig. 1. To author's knowledge, this is the first demonstration of a multi-mode sub-THz interconnect channel. The orthomode signals are fed by two pairs of differential microstrip probes. The modes  $E_{y11}$  and  $E_{x11}$  can be propagated in the DWG simultaneously with good isolation.

## II. ORTHOMODE CHANNEL DESIGN

Fig. 1(a) and (b) show the orthomode sub-THz channel, consisting of a straight DWG, and two back-to-back OMTs. Each transition includes two pairs of differential microstrip probes orthogonally, which can suppress the common mode and reduce the radiation loss, and a quarter-wavelength DWG with a metal reflector, which serves for the out-of-phase signal cancellation. The microstrip probes are perpendicular with the propagation direction of the EM waves in the DWG. To match the impedance between MSL and DWG, the microstrip probe size is designed as  $20\ \mu\text{m} \times 200\ \mu\text{m}$ . Since the center operation frequency is set at 165 GHz, the length of a side of DWG is  $500\ \mu\text{m}$  [3]. The center opening of the ground has the same size with the DWG to assist the out-of-phase cancellation. The quarter wavelength in silicon is about  $130\ \mu\text{m}$  at 165 GHz. The  $50\text{-}\Omega$  MSL is designed on a  $20\text{-}\mu\text{m}$  BCB substrate with a metal width of  $56\ \mu\text{m}$ . Fig. 1(c) and (d) plot the simulated magnitudes of the  $E_{y11}$  and  $E_{x11}$ , respectively. The differential inputs are used for excitations, which can suppress the common mode and reduce the radiation loss. As shown in Fig. 2, the simulated minimum insertion losses for both mode  $E_{y11}$  and  $E_{x11}$  are 2.6 dB with 47.7 GHz 3-dB bandwidth. The simulated  $S_{41}$  is better than  $-30\ \text{dB}$  in the range of 140-200 GHz and the  $S_{21}$  is better than  $-20\ \text{dB}$  in the range of 144.8-186.7 GHz.

To facilitate the measurement, a planar rectangular rat-race balun is employed to convert the differential signals to single-ended. Fig. 3 illustrates the layout of the back-to-back baluns with labeled dimensions. With the characteristic impedance of  $70\ \Omega$ , the line width of the balun is  $34\ \mu\text{m}$ . The ratio of the width and length is 1:2 to form the  $180^\circ$  phase difference at center frequency. A width of  $295\ \mu\text{m}$  and a length of  $680\ \mu\text{m}$  is chosen for optimal performance. The simulated minimum insertion loss is 1.4 dB.

The complete orthomode sub-THz channel for the planar chip-to-chip communications is illustrated in Fig. 4. An overpass trace and two vias are used to allow line cross-overs, which are introduced by the two pairs of the differential-to-single-ended convertors drawn orthogonally. To maintain the symmetry of the differential inputs, a dummy overpass trace and two vias are used in the pass without cross-over as shown in Fig. 4(b). The size of the vias is  $40\ \mu\text{m} \times 40\ \mu\text{m}$  with a  $10\text{-}\mu\text{m}$  depth. The width and length of the overpass trace are  $28\ \mu\text{m}$  and  $200\ \mu\text{m}$ , respectively. The bending structure with  $400\text{-}\mu\text{m}$  radius is designed to minimized the bending loss [3]. Besides, to simplify the package complexity and strength the mechanical reliability, a  $400\text{-}\mu\text{m}$  wide,  $100\text{-}\mu\text{m}$  deep backside trench is designed instead of the tiny HRS stub ( $500\ \mu\text{m} \times 500\ \mu\text{m}$ ). In addition, joined HRS and BCB substrates are utilized instead of two separate substrates to simplify the fabrication.

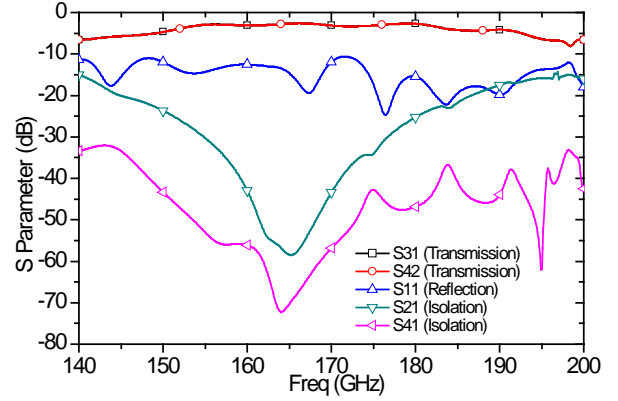


Fig. 2. Simulated S-parameters of the DWG based multi-mode sub-THz interconnect channel with the length of 8 mm.

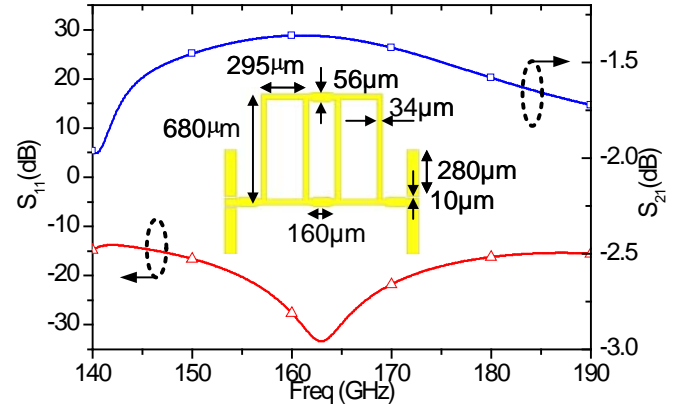


Fig. 3. Simulated S-parameters of back-to-back rectangular rat-race baluns. Dimensions of the balun are labeled in the schematic inside.

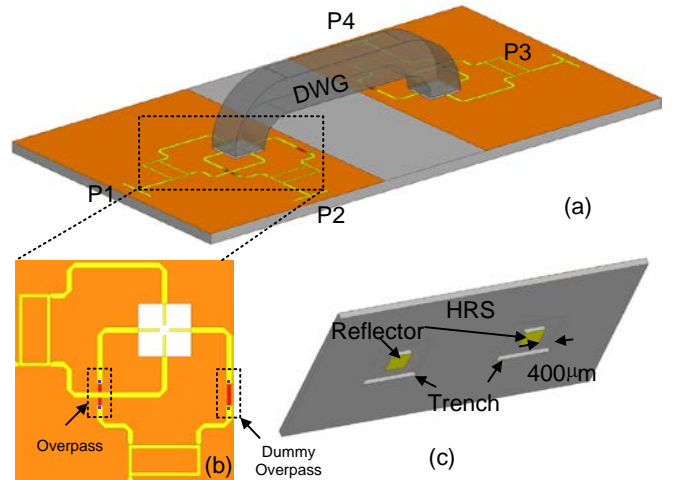


Fig. 4. (a) Perspective view of the top side of the orthomode channel, (b) the zoomed-in coupling structure, and (c) the perspective view of the back side of the orthomode channel.

## III. EXPERIMENT AND DISCUSSION

The fabrication processes are summarized in Fig. 5. BCB 4026-57 ( $\epsilon_r = 2.65$ ,  $\tan\delta = 0.015$  [7]) is used for thin-film substrate. The coupling structure includes 3 metal layers and 2 dielectric layers. Metal1 ( $20\ \text{nm}/100\ \text{nm}$  Ti/Au) is deposited on the top of a  $130\text{-}\mu\text{m}$  HRS. After that, a  $10\text{-}\mu\text{m}$  BCB is

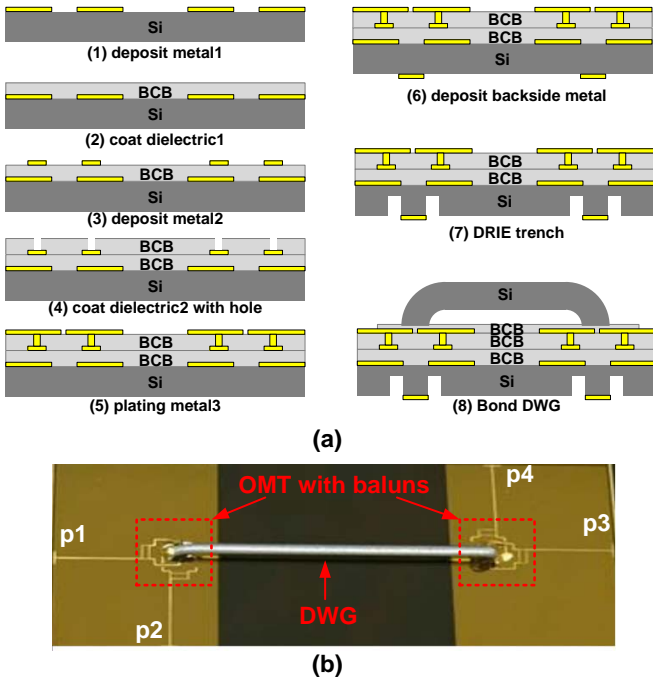


Fig. 5. (a) Fabrication procedure, and (b) photo of the top side of the orthomode channel.

spincoated with curing. And then, Metal2 (20 nm/100 nm Ti/Au) is deposited on the dielectric1. Then, a second 10- $\mu$ m BCB is spincoated and developed to form Dielectric2 with holes followed by the electrical-plating for Metal3 (2- $\mu$ m Au). After Metal3 metallization, the HRS is flipped to deposit the backside metal (20 nm/100 nm Ti/Au). Finally, the trenches around reflector is etched by deep reactive ion etching (DRIE) in a similar process as presented in [3]. With the prepared multi-mode DWG and the coupling structure, pick-and-place tool (Finetech) is used to bond the DWG to the coupling structure by 5- $\mu$ m BCB.

The measurement setup consists of an Agilent network analyzer (PNA-X N5247A), a pair of Virginia Diodes frequency extension modules (VDI WR5.1-VNAX), WR-5 (140-220 GHz) S-bend waveguides, and a pair of WR-5 probes. The SOLT (Short, Open, Load, Thru) calibration method is employed to set the reference plane at the probe tip. To characterize the channel performance, a 3.1 mm MSL with CPW-to-MSL transition at each port is de-embedded. The measured interconnect path includes an 8-mm DWG channel, two OMTs, four baluns and four 1.7-mm MSLs between the microstrip probe and the corresponding balun. Limited by the equipment, only two ports are connected each time while the other two ports are floated due to the good isolation between the orthogonal paths.

Fig. 6 plots the simulated and measured results. The measured minimum insertion losses for mode  $E_{y11}$  and mode  $E_{x11}$  are 8.0 dB with 21.3 GHz 3-dB bandwidth and 9.0 dB with 24.0 GHz 3-dB bandwidth, respectively. The isolation is better than 22 dB in the range of 140-190 GHz. The performance will be further improved by using thicker metal traces or integrated with the active devices to minimize the

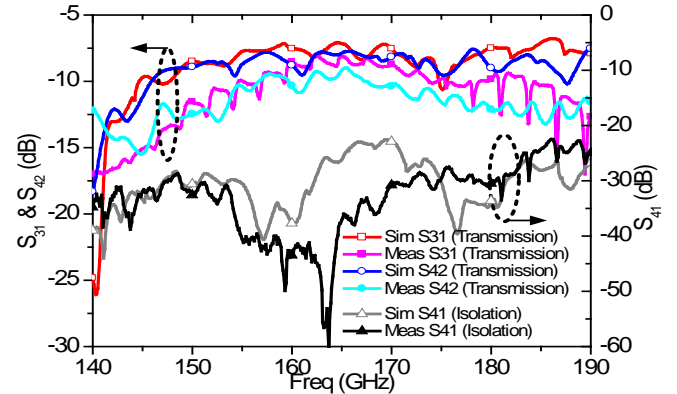


Fig. 6. Comparisons of the simulated and measured S-parameters for the orthomode channel with the length of DWG of 8 mm.

feeding line length, as well as removing the balun through differential signal generations.

#### IV. CONCLUSION

This paper for the first time presents and demonstrates a DWG based multi-mode sub-THz/THz interconnect channel. This approach opens a new direction for low-loss, wide-bandwidth, and high data-rate chip-to-chip communications. The performance will be further improved and more multi-modes can be shared in the same physical waveguide to boost the bandwidth density. In addition, this technique can be readily scaled up to THz frequencies for a better energy efficiency and bandwidth density at higher frequencies.

#### REFERENCES

- [1] X. Zheng and A. V. Krishnamoorthy, "Si photonics technology for future optical interconnection," in *Communications and Photonics Conference and Exhibition, 2011. ACP. Asia*, 2011, pp. 1–11.
- [2] E. Kadic, K. Mahajan, and A. DeHon, "Kung Fu Data Energy - Minimizing Communication Energy in FPGA Computations," in *2014 IEEE 22nd Annual International Symposium on Field-Programmable Custom Computing Machines (FCCM)*, 2014, pp. 214–221.
- [3] B. Yu, Y. Liu, Y. Ye, J. Ren, X. Liu, and Q. J. Gu, "High-Efficiency Micromachined Sub-THz Channels for Low-Cost Interconnect for Planar Integrated Circuits," *IEEE Trans. Microw. Theory Tech.*, vol. 64, no. 1, pp. 96–105, Jan. 2016.
- [4] B. Yu, Y. Liu, Y. Ye, X. Liu, and Q. J. Gu, "Low-loss and Broadband G-Band Dielectric Interconnect for Chip-to-Chip Communication," *IEEE Microw. Wirel. Compon. Lett.*, vol. 26, no. 7, pp. 478–480, Jul. 2016.
- [5] A. M. Boifot, E. Lier, and T. Schaug-Pettersen, "Simple and broadband orthomode transducer (antenna feed)," *Antennas Propag. IEE Proc. H - Microw.*, vol. 137, no. 6, pp. 396–400, Dec. 1990.
- [6] R. W. Jackson, "A planar orthomode transducer," *IEEE Microw. Wirel. Compon. Lett.*, vol. 11, no. 12, pp. 483–485, Dec. 2001.
- [7] H. M. Heiliger, M. Nagel, H. G. Roskos, H. Kurz, F. Schnieder, and W. Heinrich, "Thin-film microstrip lines for MM and sub-MM/wave on-chip interconnects," in *1997 IEEE MTT-S International Microwave Symposium Digest, 1997*, vol. 2, pp. 421–424 vol.2.